Science of the Total Environment 643 (2018) 1166–1177

Contents lists available at ScienceDirect

Science of the Total Environment

journal homepage: www.elsevier.com/locate/scitotenv

Effect partition of climate and catchment changes on runoff variation at the headwater region of the Yellow River based on the Budyko complementary relationship

Yutong Zheng [b,*], Yuefei Huang [a,b,**], Sha Zhou [b,c], Keyi Wang [b], Guangqian Wang [a,b]

[a] State Key Laboratory of Plateau Ecology and Agriculture, Qinghai University, Xining, Qinghai 810016, China
[b] State Key Laboratory of Hydroscience and Engineering, Tsinghua University, Beijing 100084, China
[c] Department of Earth and Environmental Engineering, Columbia University, NY, New York 10027, USA

HIGHLIGHTS

- The effect of climate and catchment changes on runoff variation can be partitioned precisely using the Complementary method.
- The change of precipitation has a positive impacts on the runoff variation, while the catchment change has a negative impacts on the runoff variation.
- Climate changes are the main reason for runoff reduction at the headwater region of the Yellow River.

GRAPHICAL ABSTRACT

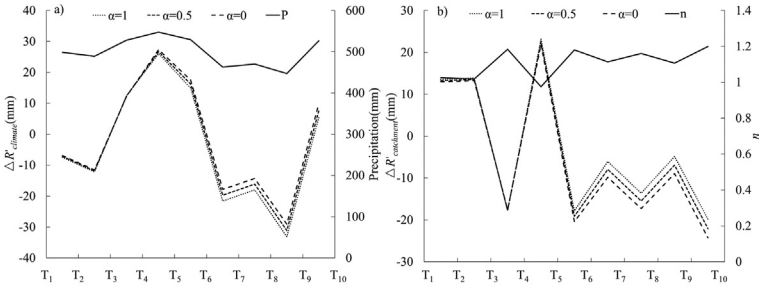

a)The changes of effect of climate changes on the runoff variation ($\triangle R'_{climate}$) and the relation between $\triangle R'_{climate}$ and Precipitation

b)The changes of effect of catchment changes on the runoff variation ($\triangle R'_{catchment}$) and the relation between $\triangle R'_{catchment}$ and catchment changes (n)

ARTICLE INFO

Article history:
Received 9 February 2018
Received in revised form 12 May 2018
Accepted 15 June 2018
Available online 4 July 2018

Editor: R Ludwig

Keywords:
Yellow River
Budyko
Runoff
Climate change
NDVI

ABSTRACT

The headwater region of the Yellow River (HRYR) is one of the most important water supply areas of the whole river basin, which has suffered a serious water shortage problem for recent years. A better understanding of impacts of climate and catchment changes on runoff variation will help to determine efficient measures to deal with the runoff reduction in the Yellow River. The Budyko complementary relationship between the partial elasticity of runoff (R) with respect to precipitation (P) and that with potential evapotranspiration (E_0) was used in this study to partition the effects of climate and catchment changes on runoff variation at the HRYR. The upper and lower bounds of the contributions of climate and catchment changes to runoff variation were determined for every five years during 1961–2010. Results show that the complementary relation method based on the Budyko hypothesis can partition the contributions of climate and catchment changes to runoff variation effectively. And the climate changes are the main reasons (account for 60%–70% of the runoff variation) for runoff reduction at the HRYR. The sensitivity coefficient of R with respect to P has a significant decreasing trend at the 0.05 level with arid ratio (E_0/P) and that with respect to E_0 has a significant increasing trend at the 0.05 level with E_0/P, indicating that with drying climate, R becomes more insensitive to climate changes. More precipitation is consumed by evapotranspiration returning to the atmosphere, leading to the runoff reduction at the HRYR.

© 2018 Elsevier B.V. All rights reserved.

* Corresponding author.
** Correspondence to: Y. Huang, State Key Laboratory of Plateau Ecology and Agriculture, Qinghai University, Xining, Qinghai 810016, China.
E-mail addresses: zhengyt2509@126.com (Y. Zheng), yuefeihuang@tsinghua.edu.cn (Y. Huang).

https://doi.org/10.1016/j.scitotenv.2018.06.195
0048-9697/© 2018 Elsevier B.V. All rights reserved.

1. Introduction

The annual change of runoff is a critical component of the hydrological cycle, and is the key to understand the water-energy balance between atmosphere and land surface (Yang et al., 2008). A number of studies have laid focus on the changing tendency of runoff across the world (Menzel and Bürger, 2002; Milly et al., 2005; Chen et al., 2006; Xu et al., 2008; S. Wang et al., 2012; Fowler et al., 2016; Huang et al., 2016). In general, the influence on annual runoff includes two aspects: direct factors and indirect factors (S. S. Wang et al., 2012). The climate changes, such as the precipitation change and the evapotranspiration change, are usually regarded as the direct ones; while the catchment changes, such as vegetation and human activates, are regarded as the indirect ones. In fact, the annual runoff is effected by the combination of both aspects for most river basins. To partition the contributions of climate and catchment changes on runoff variation quantitatively is very important for ecological restoration and policy-making in ecological fragile areas. Only the exact contribution of climate changes and catchment changes for runoff change is available, can the scientific policies and opinions on engineering measures be proposed. Thus, it is of great significance to partition the climate and catchment effects on annual runoff for the hydrological research.

Two methods were used to investigate the climate and catchment effects on runoff processes (Xu and Singh, 2004), including the hydrological modeling method and the water balance method based on Budyko hypothesis. For example, the Variable Infiltration Capacity (VIC) model was introduced to analyze the contribution of climate changes and human activities to the streamflow changes in the Haihe River Basin (Bao et al., 2012). The results showed that the decrease of streamflow could be attributed to 58.5%, 40.1%, and 26.1% from climate variability in the Taolinkou, Zhangjiafen and Guantai catchments, respectively. And the rest of the change was contributed by human activities. Wang et al. (2006) used SIMHYD model to distinguish the effect of climate changes and human activities on runoff quantitatively. The results indicated that human activities were the main reasons (64.1%) of runoff reduction in the Fenhe River basin. Although the hydrological model might be a useful tool to partition the climate changes and human activities effects on the runoff changes, many uncertainties, such as unavoidable errors, model parameters calibration, absence of partial physical processes of hydrological cycle, and disadvantages of model structure, will affect the result's accuracy (Bao et al., 2012).

Except for hydrological model, the water balance model based on Budyko hypothsis has been widely used in recent years to partition the contribution of climatic variables and catchment characteristics to runoff change. Using the precipitation (P) to represent available water, and potential evapotranspiration (E_0) to represent available energy, a general expression for the Budyko hypothesis considering the effects of both climate and catchment characteristics is:

$$\frac{E}{P} = F\left(\frac{E_0}{P}, c\right) \tag{1}$$

where $\frac{E}{P}$ is the evapotranspiration ratio, $\frac{E_0}{P}$ is the aridity index, and parameter c is used to represent different catchment characteristics, which describes a set of Budyko curves (Yang et al., 2008). Two widely used Budyko Functions are Mezentsev-Choudhury-Yang's (MCY) function (Mezentsev, 1955; Choudhury, 1999; Yang et al., 2008):

$$\frac{E}{P} = \frac{\frac{E_0}{P}}{\left[1 + \left(\frac{E_0}{P}\right)^n\right]^{1/n}} \tag{2}$$

and Fu's function (Fu, 1981):

$$\frac{E}{P} = 1 + \frac{E_0}{P} - \left[1 + \left(\frac{E_0}{P}\right)^\omega\right]^{1/\omega} \tag{3}$$

where parameters n and ω represent the catchment characteristics, such as human activities, relative infiltration capacity, vegetation coverage, soil properties, average slope and agricultural activity (H.B. Yang et al., 2012; Xing et al., 2018). Taking the MCY function as an example, the state space (E_0/P, E/P) is the solution space of the mean annual water-energy balance equation, represented by a set of Budyko curves with a constant n for a certain catchment, shown as Fig. 1.

The climate elasticity of runoff proposed by Schaake (1990) is considered to be a useful tool in the study of identifying the temporal variability of runoff to climate changes (Dooge, 1992; Dooge et al., 1999; Sankarasubramanian et al., 2001). By assuming that P, E_0, and c were independent with each other in Eq. (1), a total differential method was proposed to assess the runoff change based on the Budyko function (Roderick and Farquhar, 2011):

$$dR = \frac{\partial R}{\partial P}dP + \frac{\partial R}{\partial E_0}dE_0 + \frac{\partial R}{\partial c}dc \tag{4}$$

The partial derivatives represent the sensitivity coefficients of R with respect to P, E_0, and c, respectively. The Eq. (4) is a general expression of the total differential method, thus the effect of catchment changes to runoff variations is represented as c which is corresponding to Eq. (1). In Eq. (4), the runoff changes induced by climate changes are calculated as $\frac{\partial R}{\partial P}dP + \frac{\partial R}{\partial E_0}dE_0$. The last term on the right side, $\frac{\partial R}{\partial c}dc$, is the runoff changes induced by catchment changes. Based on Eqs. (2) and (4), X. Xu et al. (2014) analyzed the dominant cause of runoff decline in the Haihe River basin. The runoff change was calculated for 33 catchments based on the elasticity of runoff. The results showed that climate and catchment changes were accountable for the runoff decrease by 26.9% and 73.1% on average, respectively.

With global warming and society development, the Yellow River has suffered serious water resources problems, leading to various ecological problems, such as riverbed elevation, soil erosion in the Loess Plateau, and ecological deterioration of the river basin. Since the Headwater Region of the Yellow River (HRYR) is one of the main runoff generation areas of the whole river basin (Liu and Chang, 2005), attention has been paid by many researchers to understand the water-energy balance in this area (Wang et al., 2010; Liang et al., 2013; Ning et al., 2017), which would be helpful to reveal the reason of runoff decrease at the HRYR. Climate elasticity method based on Budyko hypothsis was ever used to assess the response of stream flow to climate and catchment changes in the HRYR (Zheng et al., 2009). However, the runoff effected by catchment changes were not directly calculated as $\frac{\partial R}{\partial c}dc$ in Eq. (4), but as the difference between the total change of runoff and the runoff

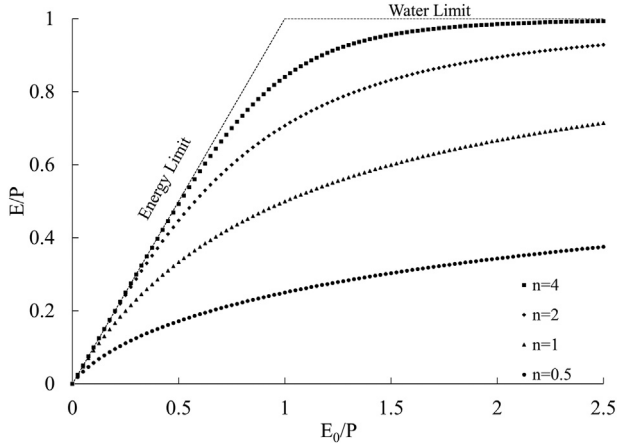

Fig. 1. Solution space for the mean annual water-energy balance equation.

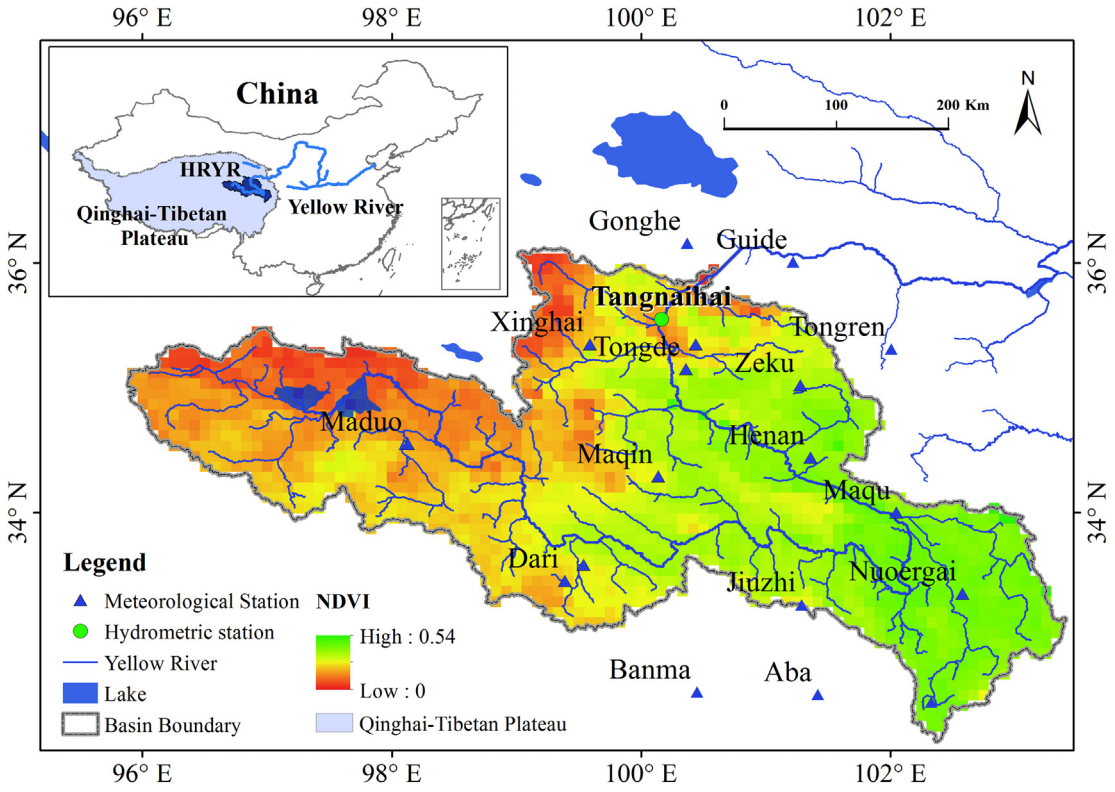

Fig. 2. Location of the headwaters region of the Yellow River.

change effected by climate changes, because of the errors associated with the climate elasticity method for practical use (Zhou et al., 2016). The results indicated that the catchment changes were responsible for >70% of the streamflow reduction in the 1990s. In addition, other studies indicated that the climate changes were the main reason for the runoff change (Li et al., 2008; Zhao et al., 2009; Zhou and Huang, 2012; Tang et al., 2013). Different analysis methods and different time series datasets resulted in significant differences among the conclusions. Therefore, it is still an unsolved issue to clearly partition the climate and catchment changes effect on runoff variation, which needs more in-depth study (Xu, 2011).

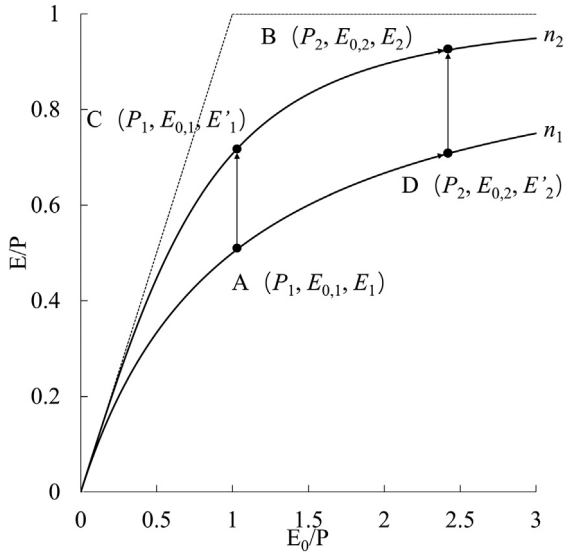

Fig. 3. The process of state space changes from initial state to final state.

The objective of this study are a) to use a new framework to partition the climate change effect and catchment change effect on runoff change quantitatively, b) to combine the sensitive coefficients, the partial elasticity of R with respect to P and E_0, with complementary relationship to calculate runoff change during the period of 1961–2010, c) to apply the new framework to the HRYR and explain reasons of runoff reduction in the HRYR.

2. Overview of study area

Located in the north-eastern part of the Qinghai-Tibet Plateau, the HRYR is one of the main areas of runoff generation in the Yellow River basin, shown as Fig. 2. The annual runoff generated from the HRYR is 2.05×10^{10} m^3, which accounts for 38% of the total runoff of the whole basin (Liu and Chang, 2005). The elevation range of the HRYR is

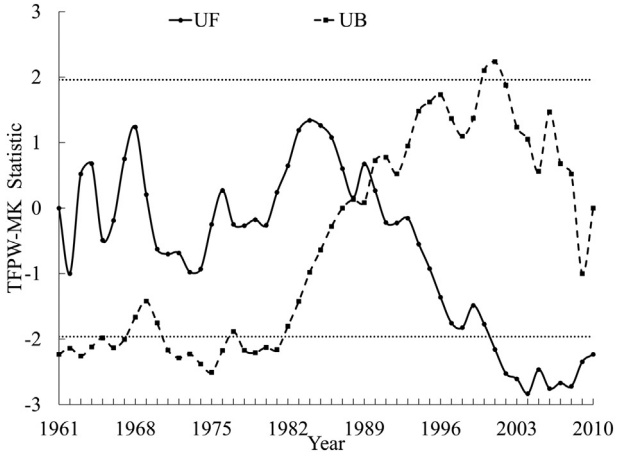

Fig. 4. The result of TFPW-MK test with forward (UF) and backward (UB). The horizontal dotted lines represent the 95% significance level (|UF| = 1.96).

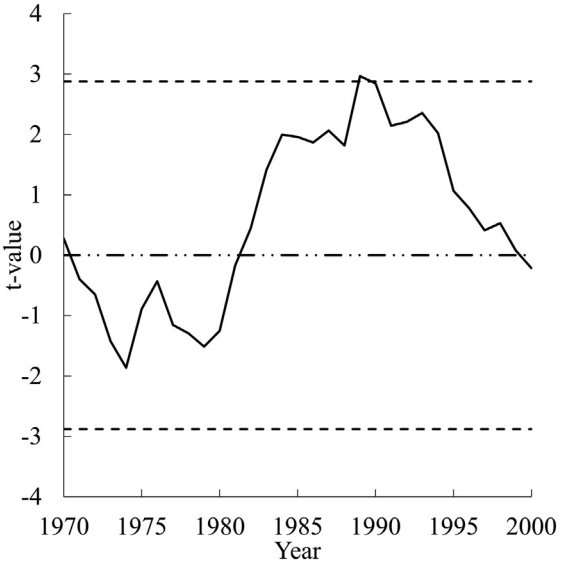

Fig. 5. T-values of moving *t*-test for the annual runoff time-series.

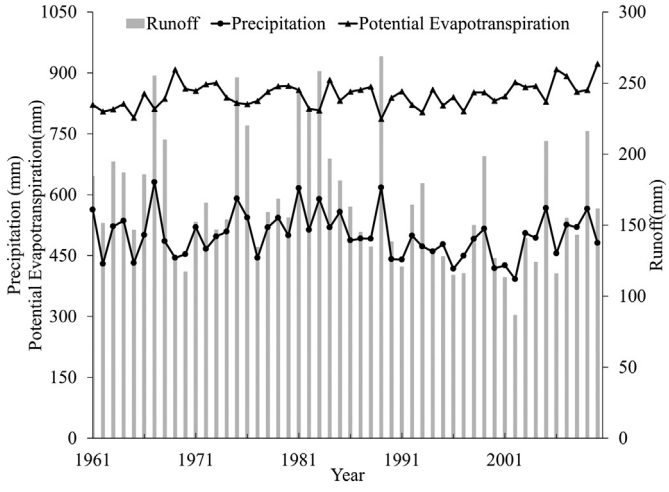

Fig. 6. Annual precipitation (P), potential evapotranspiration (E_0) and runoff (R) of the HRYR.

from 3480 m to 4680 m. From the Tangnaihai gauge station to the headstream, the river length is 1553 km, which accounts for 28.4% of the whole length of the Yellow River. The region area is 121,972 km^2, which accounts for 16.2% of the whole Yellow River Basin. For the past 50 years, the annual average precipitation was 500.20 mm, approximately 90% of which occurring from June to September, and the annual average temperature was 0.55 °C (Xu and He, 2006). Moreover, there is a significant difference in the spatial distribution of precipitation at the HRYR since the annual average precipitation at north-western part is only 200 mm, but 700 mm of that at the south-eastern part (Li et al., 2015). The distribution of the Normalized Difference Vegetation Index (NDVI), which reflects the vegetation coverage, also has the same characteristics. The annual average NDVI varies from 0 to 0.54, decreasing from south-eastern to north-western part.

3. Methodology and data

3.1. Data sources

Most of datasets used in this study including precipitation, maximum temperature, minimum temperature, relative humidity, wind speed, and radiation were obtained from open access websites such as China Meteorological Data Service Center (http://data.cma.cn/). Considering the changes in potential evapotranspiration present large spatial variability in the HRYR (W. Wang et al., 2012), FAO-Penman-Montieth (FAO-PM) equation was used to estimate the potential evapotranspiration of the HRYR. FAO-PM equation was widely used in the hydrology and meteorology, and the details of the FAO-PM equation could be found in Wang et al. (2016). Firstly, several 0.5° grid datasets (1961–2010) covering the whole China were interpolated from the meteorological datasets (precipitation, maximum temperature, minimum temperature, relative humidity, wind speed and radiation) collected from 756 stations of the whole China. Then the datasets of the study area were extracted from the 0.5° grid datasets obtained before. At last, potential evapotranspiration was estimated for each grid by FAO-PM equation. The average value of each variable for all grids within study area was calculated as the value of the whole study area. The 1961–2010 annual runoff data at the Tangnaihai gauge station was provided by Qinghai Hydrology and Water Resources Investigation Bureau. By assuming that the annual change in soil moisture content is negligible in the HRYR, the annual evapotranspiration can be obtained through calculating the difference between annual precipitation and annual runoff (Yang et al., 2007):

$$E = P - R \tag{5}$$

The annual GIMMS (Global Inventory Modelling and Mapping Studies) AVHRR (Advanced Very High Resolution Radiometer) NDVI datasets (1982–2010) had a spatial resolution of 8 km, collected from the NASA Earth Exchange (https://nex.nasa.gov/nex/). The spatial resolution of NDVI data was also resampled to 0.5° by ArcGIS resample tool.

3.2. Methodology

3.2.1. Complementary relationship method

Based on the Budyko hypothesis, Zhou et al. (2016) proposed a complementary method to partition climate and catchment effects on mean annual runoff. Assuming that P and E_0 are independent with each other, the complementary relation between the partial elasticity of R with respect to P and that with respect to E_0 is obtained (Zhou et al., 2015):

$$\frac{\partial R/R}{\partial P/P} + \frac{\partial R/R}{\partial E_0/E_0} = 1 \tag{6}$$

Then the Eq. (6) can be easily transformed into

$$R = \frac{\partial R}{\partial P}P + \frac{\partial R}{\partial E_0}E_0 \tag{7}$$

Table 1
Climate variations and basin characteristics of the HRYR.

Years	Average P (mm)	Change (%)	Average E_0 (mm)	Change (%)	Average R (mm)	Change (%)	R_c	Change (%)	n	Change (%)
1961–1989	515.84	N/A	840.95	N/A	182.36	N/A	0.35	N/A	1.06	N/A
1990–2010	476.94	−7.54%	852.07	1.32%	144.51	−20.76%	0.30	−14.29%	1.15	7.52%
1961–2010	500.20	−3.03%	845.61	0.56%	166.47	−8.71%	0.33	−5.71%	1.10	3.06%

Table 2
Average evapotranspiration (E), potential evapotranspiration (E_0), precipitation (P), runoff (R) and parameter n in Eq. (5) for each sub-period.

Sub-periods	Year range	Corresponding runoff	E (mm)	E_0 (mm)	P (mm)	R (mm)	n
T_1	1961–1965	R_1	329.91	810.28	502.07	172.76	1.10
T_2	1966–1970	R_2	319.86	853.28	498.67	178.81	1.03
T_3	1971–1975	R_3	314.73	853.77	489.18	174.45	1.02
T_4	1976–1980	R_4	360.74	848.59	528.16	167.42	1.18
T_5	1981–1985	R_5	325.61	838.42	547.64	222.03	0.97
T_6	1986–1990	R_6	359.47	840.89	529.36	169.89	1.18
T_7	1991–1995	R_7	317.61	831.56	462.71	145.10	1.11
T_8	1996–2000	R_8	329.22	836.19	470.38	141.16	1.16
T_9	2001–2005	R_9	312.37	856.19	447.11	134.74	1.11
T_{10}	2006–2010	R_{10}	368.45	887.01	526.76	158.32	1.20

where $\frac{\partial R}{\partial P}$ and $\frac{\partial R}{\partial E_0}$ are the sensitivity coefficients of R with respect to P and E_0, which can be calculated from Eqs. (2) and (5):

$$\frac{\partial R}{\partial P} = 1 - \frac{E_0}{\left(P^n + E_0^n\right)^{(1/n)}} + \frac{P^n E_0}{\left(P^n + E_0^n\right)^{(1+1/n)}} \tag{8}$$

and

$$\frac{\partial R}{\partial E_0} = \frac{P E_0^n}{\left(P^n + E_0^n\right)^{(1+1/n)}} - \frac{P}{\left(P^n + E_0^n\right)^{(1/n)}} \tag{9}$$

Based on the complementary relation for runoff (Eq. (7)), the complementary method is proposed to calculate the change of runoff.

$$dR = \frac{\partial R}{\partial P} dP + \frac{\partial R}{\partial E_0} dE_0 + d\left(\frac{\partial R}{\partial P}\right) P + d\left(\frac{\partial R}{\partial E_0}\right) E_0 \tag{10}$$

Compared with the total differential method (Eq. (4)), it can be seen that the first two terms on the right side of Eq. (10), $(\frac{\partial R}{\partial P} dP + \frac{\partial R}{\partial E_0} dE_0)$, are identical to that in Eq. (4), representing the contribution of climate changes to the change of runoff. The last two terms on the right side of Eq. (10), $(d(\frac{\partial R}{\partial P})P + d(\frac{\partial R}{\partial E_0})E_0)$, are equal to $(\frac{\partial R}{\partial c} dc)$ in the total different method, which has been demonstrated by Zhou et al. (2016), representing the contribution of catchment changes to runoff variation.

Let the initial state be $(P_1, E_{0,1}, E_1)$ and the final state be $(P_2, E_{0,2}, E_2)$ in the state space (P, E_0, and E). From the initial state to the final state, the sensitivity coefficients $(\frac{\partial R}{\partial P})_1$ and $(\frac{\partial R}{\partial E_0})_1$ change to $(\frac{\partial R}{\partial P})_2$ and $(\frac{\partial R}{\partial E_0})_2$, and the runoff and catchment characteristics parameter change from R_1 and n_1 to R_2 and n_2, respectively, shown as Fig. 3. The partitioning of the contribution of climate changes and that of catchment changes varies along different paths in the Fig. 3.

For example, the change of runoff (ΔR) can be calculated as:

$$\Delta R = \left(\frac{\partial R}{\partial P}\right)_1 \Delta P + \left(\frac{\partial R}{\partial E_0}\right)_1 \Delta E_0 + P_2 \Delta\left(\frac{\partial R}{\partial P}\right) + E_{0,2} \Delta\left(\frac{\partial R}{\partial E_0}\right) \tag{11}$$

or

$$\Delta R = \left(\frac{\partial R}{\partial P}\right)_2 \Delta P + \left(\frac{\partial R}{\partial E_0}\right)_2 \Delta E_0 + P_1 \Delta\left(\frac{\partial R}{\partial P}\right) + E_{0,1} \Delta\left(\frac{\partial R}{\partial E_0}\right) \tag{12}$$

based on the complementary relation (Zhou et al., 2016). Eq. (11) uses the initial state of sensitivity coefficients as reference to calculate the contribution of climate changes (the first two terms on the right side of Eq. (11)) and the final state of P and E_0 as reference to calculate the contribution of catchment changes (the last two terms on the right side of Eq. (11)), corresponding to the path A-D-B. And Eq. (12) uses the final state of sensitivity coefficients as reference to calculate the contribution of climate changes and the initial state of P and E_0 as reference to calculate the contribution of catchment changes, corresponding to the path A-C-B. Both of these two equations are proved to be algebraic identities (Zhou et al., 2016).

As for the uncertainty of the climate conditions and catchment characteristics, there are countless paths from the initial state to the final state, and path A-D-B and A-C-B are the boundary of these paths. Thus, the weight factor α is introduced to represent different paths from the initial state to the final state. ΔR can be expressed as a linear combination of Eq. (11) and Eq. (12), as:

$$\begin{aligned}\Delta R = {} & \alpha\left[\left(\frac{\partial R}{\partial P}\right)_1 \Delta P + \left(\frac{\partial R}{\partial E_0}\right)_1 \Delta E_0 + P_2 \Delta\left(\frac{\partial R}{\partial P}\right) + E_{0,2} \Delta\left(\frac{\partial R}{\partial E_0}\right)\right] \\ & + (1-\alpha)\left[\left(\frac{\partial R}{\partial P}\right)_2 \Delta P + \left(\frac{\partial R}{\partial E_0}\right)_2 \Delta E_0 + P_1 \Delta\left(\frac{\partial R}{\partial P}\right) + E_{0,1} \Delta\left(\frac{\partial R}{\partial E_0}\right)\right]\end{aligned} \tag{13}$$

where the weight factor α varies from 0 to 1. ΔR can be calculated as,

$$\Delta R = \Delta R_{climate} + \Delta R_{catchment} \tag{14}$$

where the $\Delta R_{climate}$ represents the contribution of climate changes,

$$\begin{aligned}\Delta R_{climate} = {} & \alpha\left[\left(\frac{\partial R}{\partial P}\right)_1 \Delta P + \left(\frac{\partial R}{\partial E_0}\right)_1 \Delta E_0\right] + (1-\alpha) \\ & \times \left[\left(\frac{\partial R}{\partial P}\right)_2 \Delta P + \left(\frac{\partial R}{\partial E_0}\right)_2 \Delta E_0\right]\end{aligned} \tag{15}$$

Table 3
$\Delta R_{climate}$ (mm) and $\Delta R_{catchment}$ (mm) with α equaling to 1, 0.5 and 0, respectively and observed and estimated ΔR (mm).

	$\Delta R_{climate}$ $\alpha = 1$	$\Delta R_{catchment}$	$\Delta R_{climate}$ $\alpha = 0.5$	$\Delta R_{catchment}$	$\Delta R_{climate}$ $\alpha = 0$	$\Delta R_{catchment}$	Observed ΔR	Estimated ΔR
ΔR_1	−7.49	13.54	−7.20	13.25	−6.91	12.96	6.05	6.05
ΔR_2	−4.69	0.33	−4.67	0.31	−4.66	0.29	−4.36	−4.36
ΔR_3	24.66	−31.70	24.24	−31.28	23.82	−30.86	−7.03	−7.03
ΔR_4	13.58	41.04	14.33	40.29	15.08	39.54	54.62	54.62
ΔR_5	−11.12	−41.02	−10.46	−41.68	−9.81	−42.33	−52.14	−52.14
ΔR_6	−36.53	11.73	−35.93	11.14	−35.34	10.55	−24.79	−24.79
ΔR_7	3.60	−7.54	3.56	−7.49	3.51	−7.44	−3.94	−3.94
ΔR_8	−15.18	8.75	−14.96	8.53	−14.73	8.31	−6.43	−6.43
ΔR_9	38.55	−14.97	38.73	−15.15	38.90	−15.32	23.58	23.58

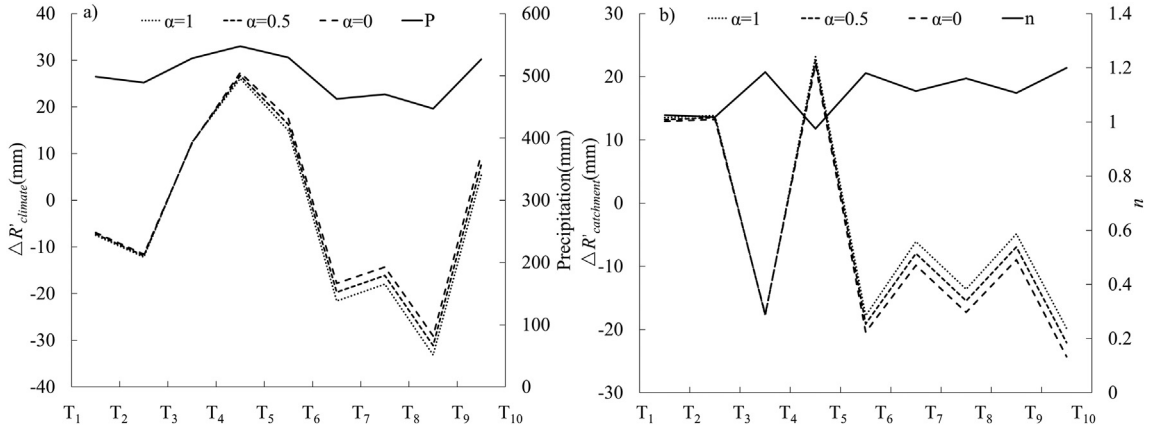

Fig. 7. a) $\Delta R'_{climate}$ changes with $\alpha = 1$, 0.5 and 0, and relation between $\Delta R'_{climate}$ and P; b) $\Delta R'_{catchment}$ changes with $\alpha = 1$, 0.5 and 0, and relation between $\Delta R'_{catchment}$ and n.

and the $\Delta R_{catchment}$ represents the contribution of catchment changes,

$$\Delta R_{catchment} = \alpha\left[P_2\Delta\left(\frac{\partial R}{\partial P}\right) + E_{0,2}\Delta\left(\frac{\partial R}{\partial E_0}\right)\right] + (1\text{-}\alpha) \times \left[P_1\Delta\left(\frac{\partial R}{\partial P}\right) + E_{0,1}\Delta\left(\frac{\partial R}{\partial E_0}\right)\right] \quad (16)$$

With the change of weight factor α, both $\Delta R_{climate}$ and $\Delta R_{catchment}$ vary linearly. Thus, when $\Delta R_{climate}$ reaches its upper bound corresponding to a specific value of α (0 or 1), the $\Delta R_{catchment}$ gets its lower bound, and vice versa. Whatever the value of α is, the sum of $\Delta R_{climate}$ and $\Delta R_{catchment}$ always equals to ΔR. The complementary method can give out the upper bound and lower bound of the contributions from both climate and catchment changes to runoff variation within the Budyko framework.

3.2.2. Changing point test

Many methods can be applied to identify the changing point of time-series (Zhang and Ge, 1990). To detect the changing point of the runoff series, the Trend-free pre-whitening Mann-Kendall test (TFPW-MK) and Moving *t*-test method were considered.

(1) TFPW-MK

The MK test is a useful tool for detecting trend and changing point (Zhai and Feng, 2009; Wang et al., 2013; Yong et al., 2013). But some studies showed that the results obtained by MK test were affect by the serial correlation and trend component (Yue et al., 2002). Through the removal of a positive serial correlation component by pre-whitening and the removal of a trend component from a time series as a first step prior to pre-whitening, the TFPW-MK can eliminate the effect of the trend on the serial correlation effectively (Yue and Wang, 2004). The TFPW-MK is calculated as following (Sen, 1968; Yue et al., 2002; Sonali and Kumar, 2013):

$$\beta = \text{median}\left(\frac{x_j - x_i}{j-i}\right), \quad \forall j<i \quad (17)$$

$$Y_t = X_t - \beta t \quad (18)$$

$$Y'_t = Y_t - rY_{t-1} \quad (19)$$

$$Y''_t = Y'_t - \beta t \quad (20)$$

where β is the slope of a trend in sample data series $\{x\}$, Y_t is the series after removing the trend component, Y'_t is the series after removing serial correlation component, r is the lag-1 correlation coefficient and Y''_t is the series obtained by TFPW process. If the lag-1 correlation coefficient is significant with the considered significant level, the TFPW process is implemented to the sample data series $\{x\}$, else the MK test is applied to the sample data series $\{x\}$ directly. The MK test is a widely used method, and the detail of MK can be found in Mann (1945) and Kendall (1975).

(2) Moving *t*-test method

Because of the mean value change can reflect the basic conditions of climate (J. X. Xu et al., 2014), the moving t-test method is used to validate the results obtained from TFPW-WK. The t-test is calculated as

$$t = \frac{\overline{x_1} - \overline{x_2}}{s\sqrt{\frac{1}{L_1} + \frac{1}{L_2}}} \quad (21)$$

and

$$s = \sqrt{\frac{L_1 s_1^2 + L_2 s_2^2}{L_1 + L_2 - 2}} \quad (22)$$

where $\overline{x_i}$ is the average values of independent samples in subseries i, s_i is the standard variation and L_i is the size of subseries i ($i = 1, 2$). The degree of freedom in the t-test is $L_1 + L_2$–2. As for the moving t-test, the t-test is applied to two subseries with fixed length L before and after potential changing point. By moving the test window, all potential

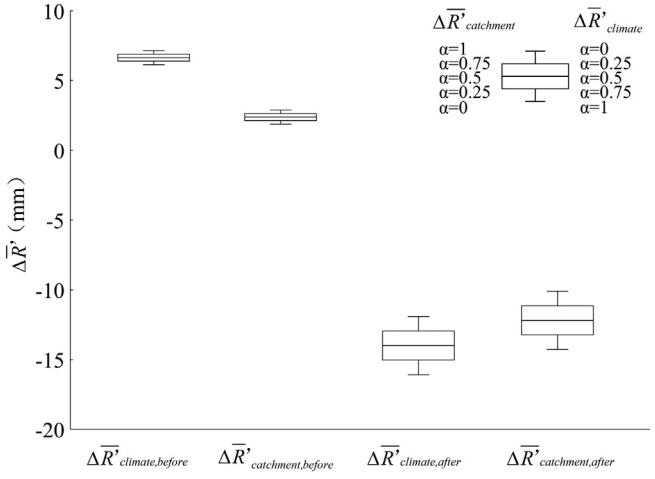

Fig. 8. Climate change and catchment change effects on runoff corresponding to $\alpha = 1$, 0.75, 0.5, 0.25 and 0 for the years 1961–1989 (before 1989) and 1990–2010 (after 1989).

Table 4
The sensitivity coefficients of R with respect to P and E_0 for each period.

Period	$\partial R/\partial P$	$\partial R/\partial E_0$
T_1	0.59	−0.15
T_2	0.59	−0.14
T_3	0.59	−0.13
T_4	0.57	−0.15
T_5	0.64	−0.15
T_6	0.57	−0.16
T_7	0.55	−0.13
T_8	0.54	−0.13
T_9	0.53	−0.12
T_{10}	0.54	−0.14

changing points will be detected. If the t-value is larger than the critical value t_α, then the corresponding point will be accepted as the changing point of the initial time-series. Moreover, the length L should not be less than five and greater than half of the sample size to ensure statistically meaningful (Zheng et al., 2010). Different L values were attempted to carry out the moving t-test. The results showed that t-values were not sensitive to the change of L. Thus, in this study, L is set to 10 and the significance level $\alpha = 0.01$ with $t_\alpha = 2.878$.

4. Results

4.1. Climate and runoff variations at the HRYR

Fig. 4 is the result of the TFPW-MK test. The intersection of the forward (UF) and backward (UB) curves indicates an abrupt change in the annual runoff (Zhang et al., 2011). From Fig. 4, it can be seen that the UF and UB curves intersect between 1989 and 1990. Thus, the years 1989 and 1990 are identified as the potential changing points of the annual runoff. Also, it can be seen that the runoff of the HRYR has a decreasing trend after 1991 (UF < 0) and the runoff shows a significant decreasing trend after 2001 (UF < −1.96).

Fig. 5 shows the result of the moving t-test. It can be seen that only the t-value of 1989 is large than t_α, indicating that the year 1989 is identified as the changing point for the annual runoff through the moving t-test method.

Based on the two changing point tests, the runoff variation can be divided into two periods: Years 1961–1989 and 1990–2010. The long-term variations in P, E_0, R, runoff coefficient (R_c) and parameter n in Eq. (2) of the HRYR from 1961 to 2010 are shown in Fig. 6 and Table 1.

From Fig. 6, it can be seen that the potential evapotranspiration has varied a little during the past 50 years (845.61 ± 29.84 mm). Both runoff and precipitation have an increasing trend during Years 1961–1989 and 1990–2010, respectively. However, they both have a decreasing trend from 1961 to 2010. In Table 1, the annual average precipitation and runoff from 1990 to 2010 decreased by 7.54% and 20.76%, respectively, compared with the Years 1961–1989. The annual average R_c for the Years 1990–2010 is 14.29% less than that for the Years of 1961–1989, indicating the change of the rainfall-runoff relation. The parameter n has increased from 1.06 to 1.15, and has a mean value of 1.10. In Fig. 1, it can be seen that a higher n indicates a higher E or a lower R for a given P and E_0.

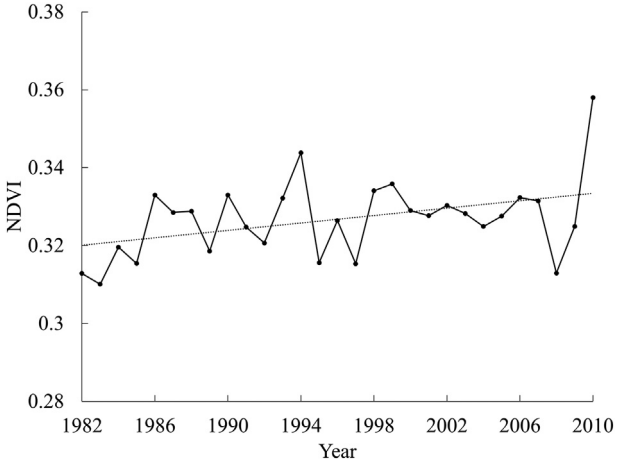

Fig. 10. the annual average NDVI in HRYR.

4.2. The runoff difference resulting from climate and catchment changes for each sub-periods

Different from the most previous studies (Zheng et al., 2009; Zhang et al., 2011; Zhou et al., 2016), in which the study period was divided into two parts, the whole period in this study is divided into ten sub-periods, and each sub-period consists of five years for tackling changing process of runoff. We assume that the change of soil moisture content is negligible between two adjacent sub-periods. Therefore, evapotranspiration can be calculated as the difference between precipitation and runoff. The climate variables and basin characteristics for each sub-period are shown in Table 2.

△R is generally defined as the difference of runoff between the final state and the initial state, referring to the difference of two adjacent sub-

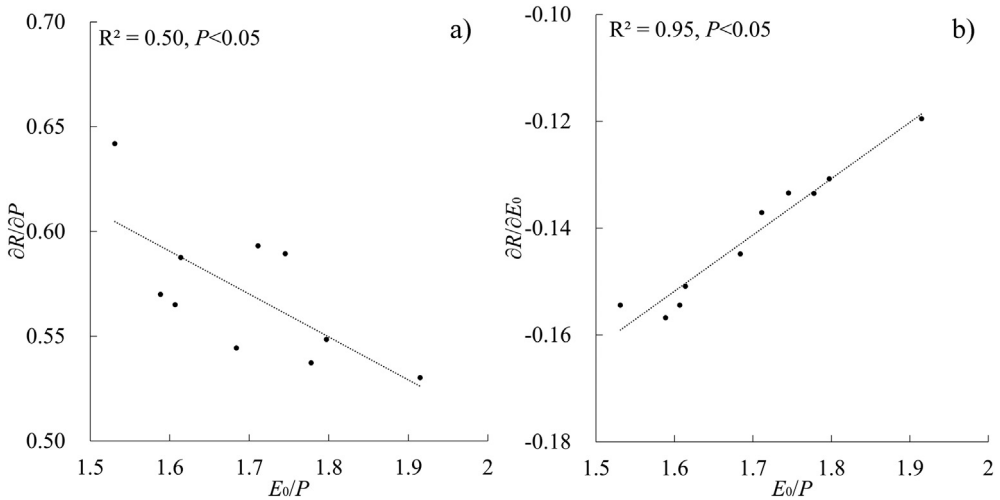

Fig. 9. a) the aridity index versus the sensitive coefficient $\partial R/\partial P$, b) the aridity index versus the sensitive coefficient $\partial R/\partial E_0$.

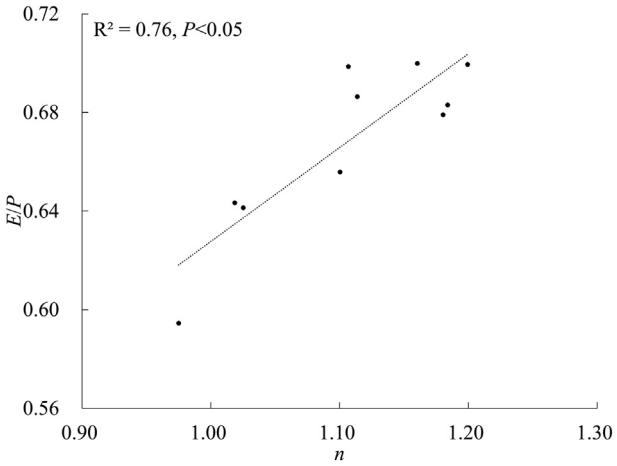

Fig. 11. Parameter *n* versus evapotranspiration index.

periods in this study, e.g., $\triangle R_1 = R_2\text{-}R_1$. The results show that the estimated $\triangle R$ is almost equal to the observed $\triangle R$, as in Table 3, indicating that the complementary method can calculate the annual runoff variation accurately. Although the sum of $\triangle R_{climate}$ and $\triangle R_{catchment}$ always equals to $\triangle R$ for one period, $\triangle R_{climate}$ and $\triangle R_{catchment}$ vary with the value of the weight factor α. Table 3 shows $\triangle R_{climate}$ and $\triangle R_{catchment}$ values with α equaling to 1, 0.5 and 0, respectively. The variation ranges of $\triangle R_{climate}$ are (−36.53, 38.55), (−35.93, 38.73), and (−35.34, 38.90) mm with α equaling to 1, 0.5 and 0, respectively. And the variation ranges of $\triangle R_{catchment}$ are (−41.02, 41.04), (−41.68, 40.29), and (−42.33, 39.54) mm with α equaling to 1, 0.5, and 0, respectively. It is different from the precious studies (Wang et al., 2006; Zheng et al., 2009; Bao et al., 2012), which assume that climate and catchment changes possess the same contribution characteristics to runoff variation. In this study, climate and catchment changes may possess the opposite contribution characteristics to runoff variation. For example, when $\alpha = 1$, $\triangle R_{climate,\ 1} = -7.49$ mm, which has a negative contribution to runoff variation, but $\triangle R_{catchment,\ 1} = 13.54$ mm, which has a positive contribution to runoff variation. $\triangle R_{climate}$ and $\triangle R_{catchment}$ in this study are both obtained from the climate elasticity of runoff (the partial

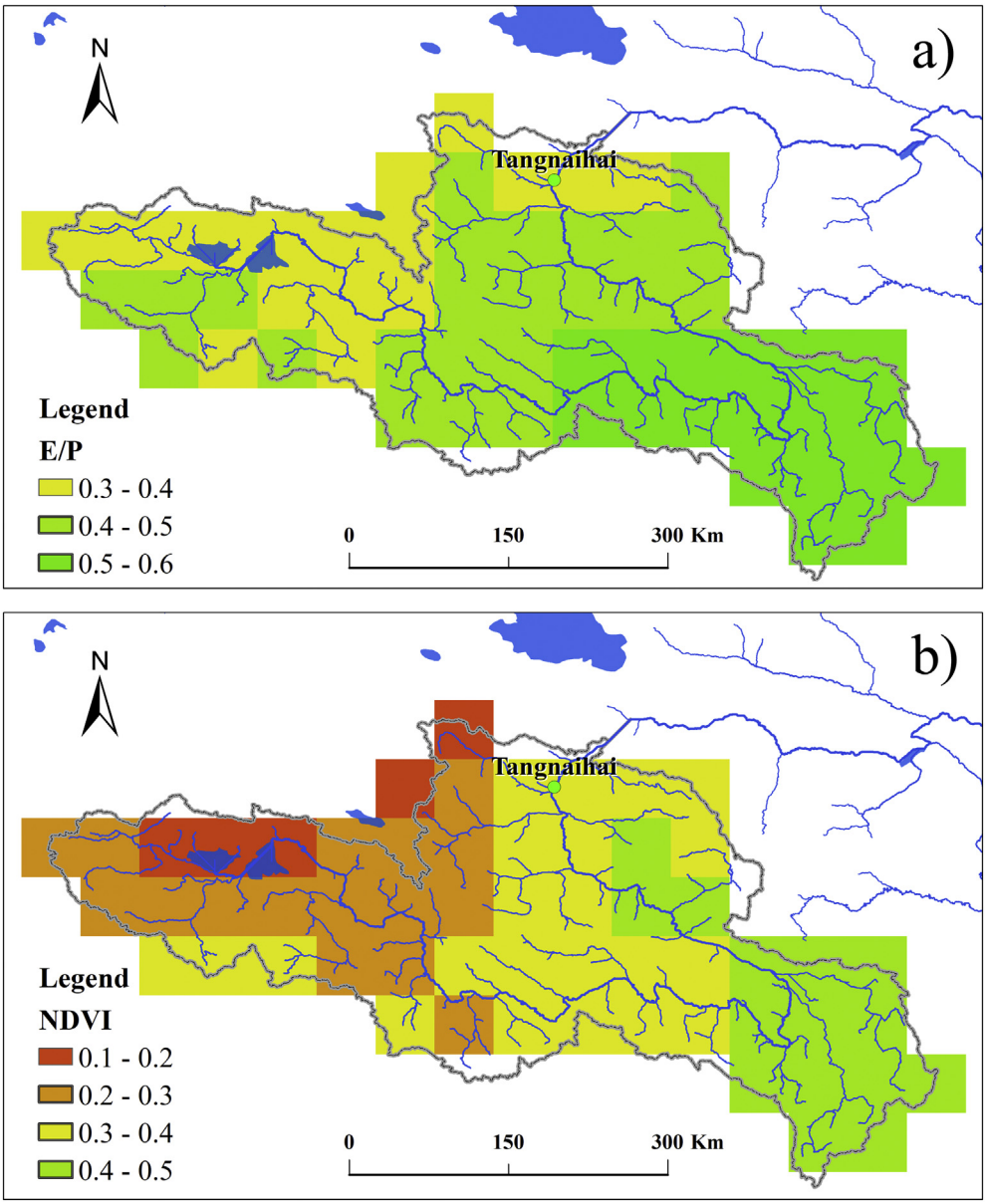

Fig. 12. a) the distribution of mean annual *E/P* of the HRYR (1982–2010); b) the distribution of mean annual NDVI of the HRYR (1982–2010).

elasticity of runoff with respect to precipitation and that with potential evapotranspiration), which is effected by the climate factors and catchment characteristics. But in the previous studies, $\triangle R_{catchment}$ is usually obtained from the difference between $\triangle R$ and $\triangle R_{climate}$.

4.3. Impacts of climate and catchment changes on runoff

Period T_1 (1961–1965) is chosen as the baseline for analyzing impacts of climate and catchment changes on runoff. $\triangle R'_{climate,i}$ and $\triangle R'_{catchment,i}$ are calculated to obtain the runoff difference between time period $i + 1$ (T_{i+1}) and time period 1 (T_1), as

$$\Delta R'_{climate,i} = \sum_{1}^{i} \Delta R_{climate,i} \tag{23}$$

$$\Delta R'_{catchment,i} = \sum_{1}^{i} \Delta R_{catchment,i} \tag{24}$$

where i is time period index ($i = 1, 2, \ldots, 9$), and $\triangle R'_{climate,i}$ and $\triangle R'_{catchment,i}$ are the runoff differences between T_{i+1} and T_1, which represent runoff affected by climate changes and catchment changes, respectively. Fig. 7 shows the $\triangle R'_{climate}$ and $\triangle R'_{catchment}$ varying with periods. It can be seen that the runoff difference between upper bound and lower bound increases over time, which may result from the error accumulation. We assumed that soil moisture content remained unchanged between the adjacent periods, which would result relatively small error for the two adjacent periods. Since the Period T_1 was chosen as the baseline, error would occur and accumulate over time. In addition, the results show that $\triangle R'_{climate}$ has a significant positive relation with P ($R^2 = 0.99$, $P < 0.05$), and $\triangle R'_{catchment}$ has a significant negative relation with n ($R^2 = 0.99$, $P < 0.05$). Obviously, P is the main driving factor of R variation, thus larger P leads to larger R, in other words, larger $\triangle R'_{climate}$. Studies have shown that the vegetation coverage can affect the infiltration and runoff generation (Cerda, 1999; Seeger, 2007). The greater the vegetation coverage is, the stronger the soil infiltration is, and the less the runoff generation is

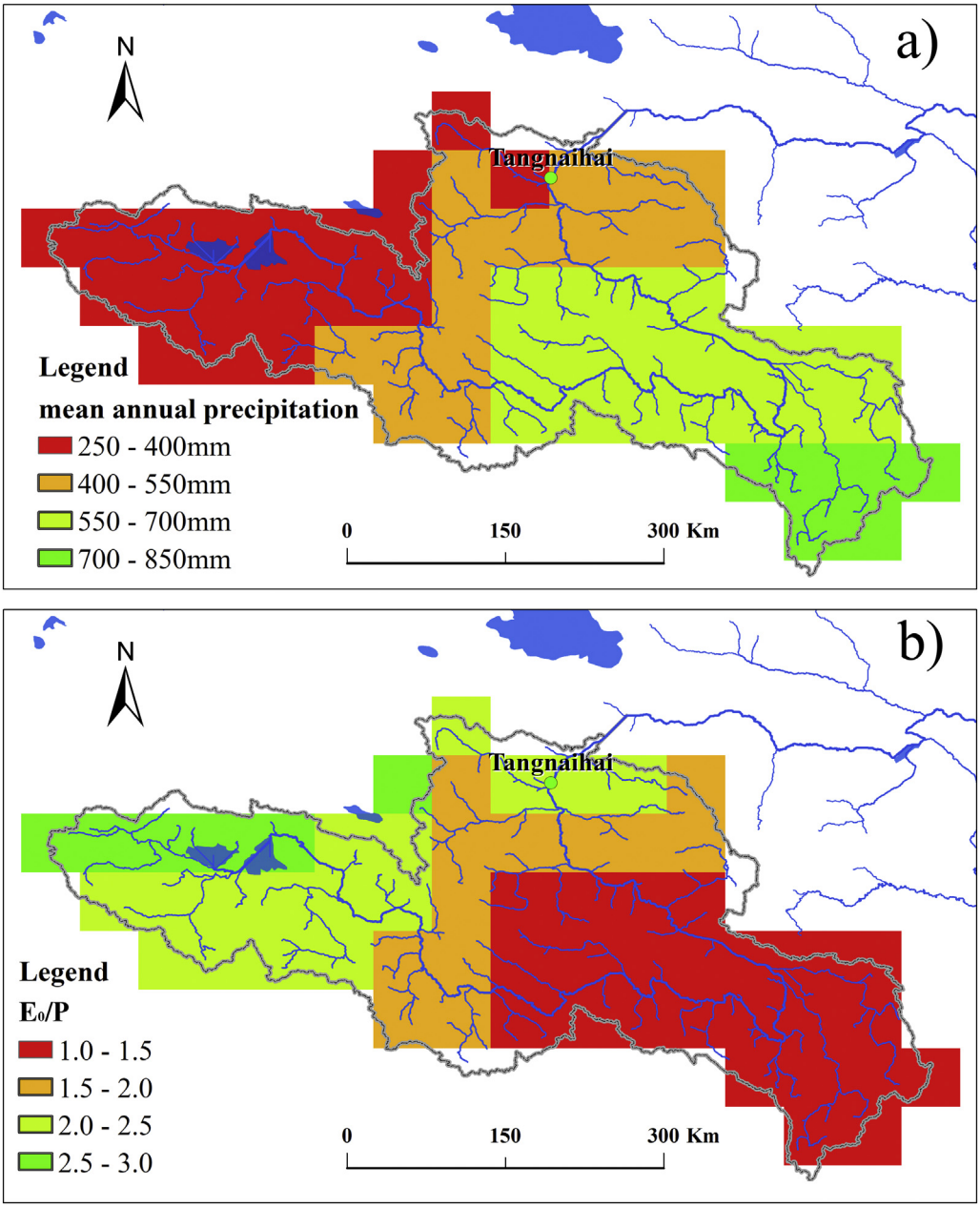

Fig. 13. a) the distribution of mean annual precipitation of the HRYR (1982–2010); b) the distribution of mean annual E_0/P of the HRYR (1982–2010).

(Zhu, 1960). Since we attribute n to vegetation coverage, the larger n indicates smaller $\Delta R'_{catchment}$, that is to say, n has.

a significant negative effect to $\Delta R'_{catchment}$.

Then the average values of $\Delta R'_{climate}$ and $\Delta R'_{catchment}$ for period before 1989 ($\Delta R'_1$, $\Delta R'_2$, $\Delta R'_3$, $\Delta R'_4$ and $\Delta R'_5$) and after 1989 ($\Delta R'_6$, $\Delta R'_7$, $\Delta R'_8$ and $\Delta R'_9$) are calculated, shown as Fig. 8. Corresponding to Fig. 7, it can be seen that the residuals for the $\Delta\overline{R}'_{climate}$ and $\Delta\overline{R}'_{catchment}$ after 1989 are larger than these of period before 1989, duo to the error accumulation. The $\Delta\overline{R}'_{climate}$ and $\Delta\overline{R}'_{catchment}$ after 1989 with negative values indicate that runoff reduction is affected by both climate and catchment changes. According to Fig. 8, climate changes play a more dominating role than that of catchment changes in affecting runoff. Before 1989, climate changes account for 69.31%, 74.23% and 79.15% of the runoff change corresponding to $\alpha = 1$, 0.5 and 0, respectively. After 1989, except for $\alpha = 0$, the climate changes are still the main reason for runoff change, but the proportion decreases a little, e.g., 60.24% and 53.09% corresponding to $\alpha = 1$ and 0.5, respectively. When $\alpha = 0$, climate changes account for 45.93% of the runoff change. The increase in E_0/P indicates the drier climate, thus, the decrease in $\Delta\overline{R}'$ for the period after 1989 may result from the increase in E_0/P and n, suggesting that more water becomes the actual evapotranspiration.

5. Discussion

5.1. Sensitivity coefficients of R with respect to climate and catchment changes

P and E_0 represent the available water and available energy at a catchment, which are the two key variables of the water-energy balance (Y. Yang et al., 2012). The parameter n, reflecting the catchment characteristics, can also affect runoff generation. As climate changes are the main reasons for runoff change, the annual precipitation decreasing by 7.09% between period 1961–1989 and period 1990–2010 results in a significant decreasing trend of runoff ($P < 0.05$) at the HRYR.

Table 4 shows the sensitivity coefficients of R with respect to P and E_0, respectively. The mean value of $\frac{\partial R}{\partial P}$ (ranging from 0.53 to 0.64) and $\frac{\partial R}{\partial E_0}$ (ranging from −0.16 to −0.12) are 0.57 and −0.14, respectively, indicating that runoff is more sensitive to P than that to E_0 at the HRYR.

It is noted that the sensitivity coefficients are not constant but vary with climate conditions. It is found that $\partial R/\partial P$ has a significant decrease trend with E_0/P ($R^2 = 0.50$, $P < 0.05$) and $\partial R/\partial E_0$ has a significant increase trend with E_0/P ($R^2 = 0.95$, $P < 0.05$), as shown in Fig. 9. It shows that sensitivity of R to P or E_0 will decrease with the increase of E_0/P.

5.2. Impacts of parameter n on runoff change

As mentioned above, $\Delta R_{catchment}$ has a significant negative correlation with parameter n. Average value of parameter n for period 1990–2010 is 7.52% more than that of period 1961–1989 (Table 1), indicating the decrease of $\Delta R_{catchment}$. Parameter n represents the catchment characteristics such as human activities, relative infiltration capacity, vegetation coverage, soil properties, average slope, climate seasonality and agricultural activity (H.B. Yang et al., 2012; Xing et al., 2018). Since the irrigated land and cultivated land were almost distributed in the north-east part of Qinghai Province (Li and Sun, 2009; Zeng et al., 2013). There were a little irrigated and cultivated land at the HRYR. Moreover, the effective irrigated ratio and cultivated land area ratio changed little in this area. Thus effect of the agricultural activity to parameter n can be ignored in this region. And the previous study also showed that parameter n could be estimated by the relative infiltration capacity, vegetation coverage and the average slope in the Yellow River basin (Yang et al., 2009). Considering that in one particular river basin, such as the HRYR, the catchment characteristics (relative infiltration capacity, soil properties, average slope, and relief ratio) can be considered constant during a certain period. Thus, in this study, it is reasonable to simply attribute catchment change to vegetation coverage change at the HRYR where it is untraversed. Fig. 10 shows the annual average NDVI at the HRYR, since the vegetation coverage can be reflected by NDVI. It can be seen that the vegetation coverage at the HRYR has an increasing trend over time, especially after the establishment of "Qinghai Three-River Headwaters Nature Reserve" in year 2010. The growth of vegetation may intercept more precipitation. Besides infiltrating into soil becoming groundwater, the intercepted water may quickly return to atmosphere through evaporation (Xu, 2011; Y. Yang et al., 2012). As shown in Fig. 11, a significant positive correlation is found between n and E/P ($R^2 = 0.70$, $P < 0.05$), indicating that the increase in vegetation coverage will increase the evapotranspiration index (E/P). Fig. 12 shows the distribution of mean annual E/P (Fig. 12(a)) and the distribution of mean annual NDVI (Fig. 12(b)) of the HRYR during 1982–2010. It can be seen that the distribution of E/P is accordance with that of NDVI. The south-eastern part of HRYR with NDVI about 0.4 has a higher evapotranspiration index than that of north-western part with NDVI about 0.2. As for the sum of evapotranspiration index and runoff coefficient equals one, the increase in evapotranspiration index means the decrease of runoff coefficient, therefore, resulting in runoff decrease even with same precipitation. That is to say, with the increase of vegetation coverage, more precipitation infiltrates into soil and then back into atmosphere through evapotranspiration, especially at the south-eastern part of the HRYR, which leads to the decrease of runoff.

5.3. Parameter n and its influencing factors

The previous studies indicated that n had a high correlation with seasonality difference between precipitation and potential evapotranspiration (H.B. Yang et al., 2012), and also, the precipitation was identified as the critical climatic factor to result in various NDVI values, especially the 2-month consecutive average precipitation at the HRYR (Zheng et al., 2017). Fig. 13 shows the distribution of mean annual precipitation and mean annual E_0/P of the HRYR. It can be seen that the area with higher precipitation values (Fig. 13(a)) corresponds with the area with higher NDVI values (Fig. 12(b)), for the precipitation can advance the growth of vegetation. The larger value of E_0/P (Fig. 13(b)) indicates a drier climate, which corresponds to the lower value of NDVI (Fig. 12(b)). Thus, the north-western part of the HRYR with higher E_0/P values correspond to the lower NDVI values.

Actually, the interconnections between parameter n and its influencing factors are complex at different spatiotemporal scale. Except for climate factors and catchment characteristics, the previous study assessed the effect of anthropogenic factors (effective irrigated area ratio and cultivated land area ratio) on parameter n quantitatively (Xing et al., 2018). The results showed that the interconnections among these influencing factors (climate, catchment and anthropogenic factors) also had potential effect on the runoff partition process. Inclusion of more influencing factors may eliminate the problems of biased sampling and reduce the uncertainty when estimating parameters of Budyko type equation (Shao et al., 2012). Thus a deeper understanding of catchment scale water balance and Budyko framework is needed for the improvement of precision for the runoff partition process in the future study.

6. Conclusion

In this study, a new method was used to partition the effect of climate and catchment changes on annual runoff variation quantitatively in the HRYR based on the Budyko complementary relationship. The effect of climate and catchment changes on annual runoff variation can be calculated through the partial elasticity of runoff with respect to precipitation and that with potential evapotranspiration directly. Another

advantage of this method compared with the previous studies, in which the study period was divided into two sub-periods, is that the whole study period can be divided into multiple sub-periods. Therefore, the effects dynamics of climate and catchment changes on runoff variations can be characterized clearly. The results show that the climate changes are the main reason (accounts for 60%–70%) for runoff reduction at the HRYR, which agree with most of the previous studies (Li et al., 2008; Zhao et al., 2009; Zhou and Huang, 2012; Tang et al., 2013). Considering the decrease in precipitation, the runoff in Tangnaihai gauge station has a decreasing trend correspondingly.

Moreover, increase in vegetation coverage may also lead to the increase in evapotranspiration and infiltration. Thus, more precipitation translates into evapotranspiration rather than runoff. With the increase of E_0/P, the runoff change is more insensitive to the change of P or E_0, also indicating that more water translates into actual evapotranspiration leading to a reduction of runoff. In this study, only three kinds of observed data are used, precipitation, potential evapotranspiration, and runoff, for the catchment. Although the runoff change cannot be divided into impacts of climate changes and catchment changes precisely, the upper and lower bound are given respectively. This method assumes that the soil moisture is constant for the long-term average. Thus, it can be used to analyze the effect of climate and catchment changes on the annual average change of runoff quantitatively for the area where the soil moisture content remains the same or changes little.

Acknowledgement

This study was financially supported by the National Natural Science Foundation of China (No.91647212). The authors would also like to thank the anonymous reviewers for their valuable comments and suggestions on the manuscript which truly improve the quality of the manuscript.

References

Bao, Z., Zhang, J., Wang, G., et al., 2012. Attribution for decreasing streamflow of the Haihe River basin, northern China: climate variability or human activities? J. Hydrol. 460–461 (3), 117–129.
Cerda, A., 1999. Parent material and vegetation affect soil erosion in eastern Spain. Soil Sci. Soc. Am. J. 63 (2), 362–368.
Chen, Y., Takeuchi, K., Xu, C., et al., 2006. Regional climate change and its effects on river runoff in the Tarim Basin, China. Hydrol. Process. 20 (10), 2207–2216.
Choudhury, B.J., 1999. Evaluation of an empirical equation for annual evaporation using field observations and results from a biophysical model. J. Hydrol. 216, 99–110.
Dooge, J.C.I., 1992. Sensitivity of runoff to climate change: a Hortonian approach. Bull. Am. Meteorol. Soc. 73 (12), 2013–2024.
Dooge, J.C.I., Bruen, M., Parmentier, B., 1999. A simple model for estimating the sensitivity of runoff to long-term changes in precipitation without a change in vegetation. Adv. Water Resour. 23 (2), 153–163.
Fowler, K.J.A., Peel, M.C., Western, A.W., et al., 2016. Simulating runoff under changing climatic conditions: revisiting an apparent deficiency of conceptual rainfall-runoff models. Water Resour. Res. 52 (3), 1820–1846.
Fu, B.P., 1981. On the calculation of the evaporation from land surface. Sci. Atmos. Sin. 5 (1), 23–31.
Huang, S., Liu, D., Huang, Q., et al., 2016. Contributions of climate variability and human activities to the variation of runoff in the Wei River Basin, China. Hydrol. Sci. J. 61 (6), 1026–1039.
Kendall, M.G., 1975. Rank Correlation Methods. Griffin, London, UK.
Li, S.Y., Sun, X.Q., 2009. Studies and analysis on dynamic changes of arable land and driving forces in the past 10 years in Qinghai Province. Chin. J. Agric. Resour. Reg. Plann. 30 (5), 39–44.
Li, L., Hao, Z.C., Wang, J.H., et al., 2008. Impact of future climate change on runoff in the head region of the Yellow River. J. Hydrol. Eng. 13 (5), 347–354.
Li, X.Y., Yao, Z.Y.., Wang, H.W., et al., 2015. Characteristics of precipitation and temperature in source region of the Yellow River in the recent 52 years. Yellow River 37 (7), 16–21.
Liang, K., Liu, C., Liu, X., Song, X., 2013. Impacts of climate variability and human activity on streamflow decrease in a sediment concentrated region in the Middle Yellow River. Stoch. Env. Res. Risk A. 27 (7), 1741–1749.
Liu, X.Y., Chang, X.H., 2005. A summary of study on runoff variations in rource region of the yellow river. Yellow River 27 (2), 6–8.
Mann, H.B., 1945. Nonparametric tests against trend. Econometrica 13 (3), 245–259.
Menzel, L., Bürger, G., 2002. Climate change scenarios and runoff response in the Mulde catchment (Southern Elbe, Germany). J. Hydrol. 267 (1), 53–64.
Mezentsev, V.S., 1955. More on the calculation of average total evaporation. Meteorol. Gidrol. 5, 24–26.
Milly, P.C.D., Dunne, K.A., Vecchia, A.V., 2005. Global pattern of trends in streamflow and water availability in a changing climate. Nature 438 (7066), 347–350.
Ning, T., Li, Z., Liu, W., 2017. Vegetation dynamics and climate seasonality jointly control the interannual catchment water balance in the Loess Plateau under the Budyko framework. Hydrol. Earth Syst. Sci. 21, 1–25.
Roderick, M.L., Farquhar, G.D., 2011. A simple framework for relating variations in runoff to variations in climatic conditions and catchment properties. Water Resour. Res. 47 (12), 667–671.
Sankarasubramanian, A., Vogel, R.M., Limbrunner, J.F., 2001. Climate elasticity of streamflow in the United States. Water Resour. Res. 37 (6), 1771–1781.
Schaake, J.C., 1990. From climate to flow, in Climate Change and U.S. Water Resources. In: Waggoner, P.E. (Ed.), chap. 8. John Wiley, New York, pp. 177–206.
Seeger, M., 2007. Uncertainty of factors determining runoff and erosion processes as quantified by rainfall simulations. Catena 71 (1), 56–67.
Sen, P.K., 1968. Estimates of the regression coefficient based on Kendall's Tau. Publ. Am. Stat. Assoc. 63 (324), 1379–1389.
Shao, Q., Traylen, A., Zhang, L., 2012. Nonparametric method for estimating the effects of climatic and catchment characteristics on mean annual evapotranspiration. Water Resour. Res. 48 (3) W03517.
Sonali, P., Kumar, D.N., 2013. Review of trend detection methods and their application to detect temperature changes in India. J. Hydrol. 476 (1), 212–227.
Tang, Y., Tang, Q., Tian, F., et al., 2013. Responses of natural runoff to recent climatic changes in the Yellow River basin, China. Hydrol. Earth Syst. Sci. 17 (11), 4471–4480.
Wang, G.Q., Zhang, J.Y., He, R.M., 2006. Impacts of environmental change on runoff in Fenhe river basin of the middle Yellow River. Adv. Water Sci. 17 (6), 853–858.
Wang, J., Hong, Y., Gourley, J., Adhikari, P., Li, L., Su, F., 2010. Quantitative assessment of climate change and human impacts on long-term hydrologic response: a case study in a sub-basin of the Yellow River, China. Int. J. Climatol. 30, 2130–2137.
Wang, S., Yan, M., Yan, Y., et al., 2012. Contributions of climate change and human activities to the changes in runoff increment in different sections of the Yellow River. Quat. Int. 282, 66–77.
Wang, W., Shao, Q., Peng, S., et al., 2012. Reference evapotranspiration change and the causes across the Yellow River Basin during 1957–2008 and their spatial and seasonal differences. Water Resour. Res. 48 (5), 113–122.
Wang, W., Shao, Q., Yang, T., et al., 2013. Quantitative assessment of the impact of climate variability and human activities on runoff changes: a case study in four catchments of the Haihe River basin, China. Hydrol. Process. 27 (8), 1158–1174.
Wang, W., Zou, S., Shao, Q., et al., 2016. The analytical derivation of multiple elasticities of runoff to climate change and catchment characteristics alteration. J. Hydrol. 541, 1042–1056.
Xing, W., Wang, W., Shao, Q., et al., 2018. Identification of dominant interactions between climatic seasonality, catchment characteristics and agricultural activities on Budyko-type equation parameter estimation. J. Hydrol. 556, 585–599.
Xu, J., 2011. Variation in annual runoff of the Wudinghe River as influenced by climate change and human activity. Quat. Int. 244 (2), 230–237.
Xu, Z.X., He, W.L., 2006. Spatial and temporal characteristics and change trend of climatic elements in the headwater region of the yellow river in recent 40 years. Plateau Meteorol. 5 (5), 906–913.
Xu, C.Y., Singh, V.P., 2004. Review on regional water resources assessment models under stationary and changing climate. Water Resour. Manag. 18 (6), 591–612.
Xu, J., Chen, Y., Ji, M., et al., 2008. Climate change and its effects on runoff of Kaidu River, Xinjiang, China: a multiple time-scale analysis. Chin. Geogr. Sci. 18 (4), 331–339.
Xu, X., Yang, D., Yang, H., et al., 2014. Attribution analysis based on the Budyko hypothesis for detecting the dominant cause of runoff decline in Haihe basin. J. Hydrol. 510 (6), 530–540.
Xu, J.X., Chen, X.K., Huang, X., 2014. Analysis of mutation characteristics of precipitation in Meitan country. J. N. China Univ. Water Resour. Electr. Power 35 (2), 6–11 (Natural Science Edition).
Yang, D., Sun, F., Liu, Z., Cong, Z., Ni, G., Lei, Z., 2007. Analyzing spatial and temporal variability of annual water-energy balance in nonhumid regions of China using the Budyko hypothesis. Water Resour. Res. 43, W04426. https://doi.org/10.1029/2006WR005224.
Yang, H., Yang, D., Lei, Z., et al., 2008. New analytical derivation of the mean annual water-energy balance equation. Water Resour. Res. 44 (3), 893–897.
Yang, D.W., Shao, W.W., Yeh, P.J.F., et al., 2009. Impact of vegetation coverage on regional water balance in the nonhumid regions of China. Water Resour. Res. 45 (7), 450–455.
Yang, Y., Shang, S., Jiang, L., 2012. Remote sensing temporal and spatial patterns of evapotranspiration and the responses to water management in a large irrigation district of North China. Agric. For. Meteorol. 164 (8), 112–122.
Yang, H.B., Lv, H.F., Yang, D.W., Hu, Q.F., 2012. Seasonality of precipitation and potential evaporation and its impact on catchment water-energy balance. J. Hydroelectric Eng. 31 (4), 54–59.
Yong, B., Ren, L., Hong, Y., et al., 2013. Spatial–temporal changes of water resources in a typical Semiarid Basin of North China over the past 50 years and assessment of possible natural and socioeconomic causes. J. Hydrometeorol. 14 (4), 1009–1034.
Yue, S., Wang, C.Y., 2004. The Mann-Kendall test modified by effective sample size to detect trend in serially correlated hydrological series. Water Resour. Manag. 18 (3), 201–218.
Yue, S., Pilon, P., Phinney, B., et al., 2002. The influence of autocorrelation on the ability to detect trend in hydrological series. Hydrol. Process. 16 (9), 1807–1829.
Zeng, Y.N., Jin, W.P., Wang, H.M., et al., 2013. Analysis and evaluation of cultivated land decrease in eastern part of Qinghai Plateau. Trans. Chin. Soc. Agric. Eng. 29 (21), 214–222.

Zhai, L., Feng, Q., 2009. Spatial and temporal pattern of precipitation and drought in Gansu Province, Northwest China. Nat. Hazards 49 (1), 1.
Zhang, P.Y., Ge, Q.S., 1990. Abrupt climatic change: introduction and a case study. Geogr. Res. 9 (2), 92–100.
Zhang, Y., Guan, D., Jin, C., et al., 2011. Analysis of impacts of climate variability and human activity on streamflow for a river basin in northeast China. J. Hydrol. 410 (3), 239–247.
Zhao, F.F., Xu, Z.X., Zhang, L., Zuo, D.P., 2009. Streamflow response to climate variability and human activities in the upper catchment of the Yellow River Basin. Sci. China Ser. E: Technol. Sci. 52 (11), 3249–3256.
Zheng, H.X., Zhang, L., Zhu, R.R., et al., 2009. Responses of streamflow to climate and land surface change in the headwaters of the Yellow River Basin. Water Resour. Res. 45 (7), 641–648.
Zheng, H., Zhang, L., Liu, C., et al., 2010. Changes in stream flow regime in headwater catchments of the Yellow River basin since the 1950s. Hydrol. Process. 21 (7), 886–893.
Zheng, Y., Han, J., Huang, Y., et al., 2017. Vegetation response to climate conditions based on NDVI simulations using stepwise cluster analysis for the Three-River headwaters region of China. Ecol. Indic. https://doi.org/10.1016/j.ecolind.2017.06.040.
Zhou, D.G., Huang, R.H., 2012. Response of water budget to recent climatic changes in the source region of the Yellow River. Chin. Sci. Bull. 57 (17), 2155–2162.
Zhou, S., Yu, B., Huang, Y., Wang, G., 2015. The complementary relationship and generation of the Budyko functions. Geophys. Res. Lett. 42, 1781–1790.
Zhou, S., Yu, B., Zhang, L., et al., 2016. A new method to partition climate and catchment effect on the mean annual runoff based on the Budyko complementary relationship. Water Resour. Res. 52 (9).
Zhu, X.M., 1960. Effects of vegetation factors on soil erosion in loess area. Acta Pedol. Sin. 8 (2), 110–121.